Carbohydrate Polymers 115 (2015) 294–304

Contents lists available at ScienceDirect

Carbohydrate Polymers

journal homepage: www.elsevier.com/locate/carbpol

Modification of arabinogalactan propargyl ethers by triazolyl functions

Lyudmila A. Grischenko[a], Lidiya N. Parshina[a], Lyudmila I. Larina[a], Lyubov N. Novikova[b], Boris A. Trofimov[a,*]

[a] A. E. Favorsky Irkutsk Institute of Chemistry, Siberian Branch of the Russian Academy of Sciences, 1 Favorsky Str., 664033 Irkutsk, Russia
[b] Irkutsk State Agricultural Academy, Molodezhny Settlement, 664038 Irkutsk, Russia

ARTICLE INFO

Article history:
Received 23 June 2014
Received in revised form 11 August 2014
Accepted 11 August 2014
Available online 27 August 2014

Keywords:
Arabinogalactan functionalization
Biopolymers
1,3-Dipolar cycloaddition
Sodium azide
Organyl halides

ABSTRACT

Polysaccharide arabinogalactan (AG) has been modified by triazolyl functions via the copper-catalyzed 1,3-dipolar addition of azides to propargyl ethers. A range of new AG triazolo derivatives bearing benzyl, 4-vinylbenzyl, 1-naphthylmethyl, (1-vinylimidazol-2-yl)methyl, (1-ethylimidazol-2-yl)methyl, (1-vinylbenzimidazol-2-yl)methyl, allyl, carboxymethyl (as Na-salt) substituents is prepared by "one-pot" approach from organic azides generated in situ and AG propargyl ethers. The latter (degree of substitution 2.0–2.2) are converted into 1,2,3-triazolo AGs in DMSO/water mixture in the presence of $CuSO_4 \cdot 5H_2O$/sodium ascorbate/Et_3N in 82–94% yields and with 60–100% conversion.

1. Introduction

Arabino-3,6-galactan (AG) is highly branched natural polysaccharide composed of galactose and arabinose. The most common commercial source of AG is the wood of larch (D'Adamo, 1990; López-Franco, Higuera-Ciapara, Goycoolea, & Wang, 2009). The water solubility, biocompatibility, biodegradability, low toxicity and easy drug conjugation in aqueous medium make AG attractive as a potential drug carrier (D'Adamo, 1990; Elgart, Farber, Domb, Polacheck, & Hoffman, 2010; Kagan et al., 2012; Pawar et al., 2011; Pinhassi et al., 2010; Polyakov, Magyar, & Kispert, 2013). Growing evidence obtained from in *vitro*, animal and human studies demonstrate the immunomodulating (D'Adamo, 1990; Dubrovina et al., 2001; Elgart et al., 2010; Pawar et al., 2011; Pinhassi et al., 2010; Riede, Grube, & Gruenwald, 2013; Udani, 2013), gastroprotective (D'Adamo, 1990; Pawar et al., 2011; Robinson, Feirtag, & Slavin, 2001), prebiotic (D'Adamo, 1990; Pawar et al., 2011; Raso et al., 2014) and antimetastatic (D'Adamo, 1990; Pawar et al., 2011) properties of AG. This polysaccharide has also attracted much interest as stabilizing matrix for the preparation of metal nanoparticles (Gasilova & Aleksandrova, 2011; Gasilova, Matveeva, Aleksandrova, Sukhov, & Trofimov, 2013; Gasilova et al., 2010; Grishchenko et al., 2006; Laurent et al., 2008; Shurygina et al., 2011; Sukhov et al., 2007; Trofimov et al., 2003), ferromagnetic agents for medical diagnosis and therapy (Aleksandrova et al., 2010; Corot, Robert, Idée, & Port, 2006; Gendler, Novakova, Prudnikov, Aleksandrova, & Grishchenko, 2009; Mahdavi et al., 2013), and catalysts (Parshina, Tantsyrev, Grishchenko, & Trofimov, 2013; Trofimov et al., 2007).

The development of new valuable products and materials based on AG can be considerably improved by its chemical modification via introduction of the reactive moieties. This approach is general for polysaccharides and its relevancy constantly grows due to the ever-increasing importance of renewable feedstock in the production of new environmentally benign materials.

Earlier, a convenient and efficient method for the synthesis of AG propargyl ethers with different degree of substitution (DS) has been developed (Grischenko et al., 2013; Trofimov, Parshina, & Grischenko, 2011). The method comprises the reaction of AG with propargyl bromide in two-phase system aqueous solution KOH-toluene. It is shown that propargyl substituents of the macromolecule readily undergo such classical reactions of terminal acetylenes as acetylene–allene isomerization or silver acetylide formation (Grischenko et al., 2013).

Recently, a Cu(I)-catalyzed 1,3-dipolar azide–alkyne cycloaddition (CuAAC) (Rostovtsev, Green, Fokin, & Sharpless, 2002; Tornøe, Christensen, & Meldal, 2002) has attracted attention owing to its experimental simplicity and convenience, high rate, and quantitative yields. This reaction has enabled a number of applications

* Corresponding author. Fax: +7 3952 419346.
E-mail address: boris_trofimov@irioch.irk.ru (B.A. Trofimov).

http://dx.doi.org/10.1016/j.carbpol.2014.08.050
0144-8617/

in synthesis (Liang & Astruc, 2011; Meldal & Tornøe, 2008), materials science (Mamidyala & Finn, 2010; Such, Johnston, Liang, & Caruso, 2012; Thirumurugan, Matosiuk, & Jozwiak, 2013), molecular biology (Mamidyala & Finn, 2010; Meldal & Tornøe, 2008; Thirumurugan et al., 2013), and medicinal chemistry (Meldal & Tornøe, 2008; Thirumurugan et al., 2013).

Over the past 10 years, polysaccharides chemistry has been strongly impacted by the CuAAC reaction. Polysaccharides have been often modified using this reaction for different purposes such as creating new materials, new therapeutic or diagnostic agents, or merely to understand the reactivity of such complex structures in terms of regioselectivity, degree of substitution (DS), cross-linking, etc. (Elchinger et al., 2011; Lallana, Riguera, & Fernandez-Megia, 2011). Also, for example, the modification of the most abundant natural polymers related AG has led to new biocomposite materials (Elchinger et al., 2011; Elchinger, Montplaisir, & Zerrouki, 2012; Enomoto-Rogers, Kamitakahara, Yoshinaga, & Takano, 2012; Peng et al., 2012), cellulose derivatives decorated with dendrons (Elchinger et al., 2011), novel solid supports for enzyme immobilization (Pohl, Michaelis, Meister, & Heinze, 2009) polyelectrolytes (Koschella, Richter, & Heinze, 2010), nanocrystals for ion exchange applications (Eyley & Thielemans, 2011), hydrogels exhibiting temperature resistance (Elchinger et al., 2011; Nakagawa, Kamitakahara, & Takano, 2012).

AG is also very abundant polysaccharide, especially in larch wood which contains quantities up to 35% of the AG in vacuoles (López-Franco et al., 2009). Presently larch wood AG is produced on an industrial scale and its market developed as food fiber and for biomedical and healthcare applications (the Swiss company Lonza Inc., Russian company Ametis, etc.). In the European Union, larch AG is admitted as food additive under code E409. The amount of AG that could be obtained from 1% of larch trees each year in the United States is 4.6 million metric tones (López-Franco et al., 2009). The industrial production of AG in Russia is provided by the technology of complex processing the of the Siberian larch (*Larix sibirica*) biomass (Babkin et al., 2007).

Due to its exceptional biochemical properties (notably, immunomodulating and membranotropic activities) AG is compared favorably from the other well known polysaccharide molecules that makes it attractive raw material for the creation of diverse preparations for medicine and pharmacology. Despite the attractive biomedical properties of AG, very few AG polymers have been synthesized. Application of click chemistry to AG could be a useful and convenient method for designing novel AG materials with controlled structures and promising properties, since the desired functional groups with triazole linkers can be introduced into AG. It is of apparent interest the introduction of carboxy and N-heteroatom groups included within triazole moieties to AG structure to design derivatives would-be polyelectrolytes and ligands capable to bind with biological metals. At present the metal complex compounds are increasingly in research focus as medicines for the socially relevant diseases, e.g. cancer, diabetics and viral infections (Mjos & Orvig, 2014). Besides, the membranotropic properties of AG are expected to impart the metal complexes enhanced biocompatibility.

The prospective area for AG triazolo derivatives application is their quaternization to form cation structures capable to conjugate the antitumor oligonucleotides, like as it known for triazolo chitozan (Gao, Zhang, Chen, Gu, & Li, 2009), besides, the conjugate's ability to penetrate the target cells could be supported with the AG membranotropism.

Such applications encouraged us to bring about Cu-catalyzed reaction between alkyne-terminated AG (AG propargyl ethers), sodium azide and organyl halides to develop new family of AG-based materials.

2. Materials and methods

2.1. General

AG propargyl ethers (DS 2.0–2.2) were prepared according to ref (Grischenko et al., 2013). AG (16 kDa) was extracted from *L. sibirica* (Babkin, Kolzunova, Medvedeva, Malkov, & Ostroukhova, 2005). AG is highly branched polysaccharide composed of galactose and arabinose units in a 6:1 ratio. Benzyl chloride, 4-vinylbenzyl chloride, 1-naphthylmethyl chloride, allyl bromide, chloroacetic acid, sodium azide, copper(II) sulfate pentahydrate, sodium ascorbate, Et_3N, sodium diethyldithiocarbamate trihydrate, cation-exchange resin Dowex 50WX8-200 were purchased from Sigma–Aldrich. 1-Ethyl-2-chloromethylimidazole hydrochloride, 1-vinyl-2-chloromethylimidazole hydrochloride, 1-vinyl-2-chloromethylbenzimidazole hydrochloride were prepared from 1-ethyl-2-hydroxymethylimidazole, 1-vinyl-2-hydroxymethylimidazole, 1-vinyl-2-hydroxymethylbenzimidazole respectively as described (Jones, 1949). 1-Ethyl-2-hydroxymethylimidazole, 1-vinyl-2-hydroxymethylimidazole, 1-vinyl-2-hydroxymethylbenzimidazole were prepared from 1-ethylimidazole, 1-vinylimidazole, 1-vinylbenzimidazole according to ref (Baikalova, Domnina, & Skvortsova, 1977). 1-Vinylimidazole, 1-ethylimidazole were purchased from Sigma–Aldrich. 1-Vinylbenzimidazole was prepared according to procedure (Shostakovsky, Skvortsova, Glazkova, & Domnina, 1969).

2.2. Instrumentation

The IR spectra (KBr) were recorded on a Bruker Vertex 70 spectrometer. The ^1H, ^{13}C NMR spectra were recorded on a Bruker 400 instrument (400.13, 100.62 MHz, respectively) in DMSO-d_6 (concentration was 10%) at a temperature of 25 °C. Chemical shifts were calibrated to the carbon resonances of the solvent (DMSO-d_6 $\delta_H = 2.5$, $\delta_C = 39.5$). 90° Pulses and an antigate sequence were the

Table 1
Conditions and results of 1,3 dipolar cycloaddition of benzyl azide (BnCl + NaN_3) to arabinogalactan propargyl ethers (DS 2.0–2.2, 1.7 mmol of C≡CH).

BnN_3, mmol (BnCl + NaN_3 = 1:1)	*T*, °C	Time, h	Conversion of C≡CH[a], %	Product		
				Sample	DS[a]	Yield, %
1.7	20–25	6	59	**1a**	1.3	91
1.7	20–25	12[b]	10	**1b**	0.2	90
1.7	20–25	12	80	**1c**	1.6	89
1.7	62–65	6	95	**1d**	2.1	87
2.7	20–25	6	90	**1e**	1.8	86
2.7	20–25	12	100	**1f**	2.1 (2.0[c])	93
2.7	62–65	6	86	**1g**	1.9	85
2.7	62–65	6	100	**1h**	2.2	89

[a] Conversion, DS determined by EA.
[b] Reaction was carried out without Et_3N. In other experiments, 1.7 mmol of Et_3N was used.
[c] DS determined by ^{13}C NMR.

proton decoupler switched off during the pulse delay. The pulse delays were 5.0 s and the number of scans ranged from 15,000 to 20,000 for ^{13}C NMR spectra.

EA was performed with a Flash EA Analyzer. The sodium, copper content of the samples was determined by the energy-dispersive X-ray microanalyses method using electron microscope Hitachi TM 3000 with X-ray detector SDD XFlash 430-H.

The weight-average molecular mass was determined by means GPC with Sephadex G-100 column (24 mm × 350 mm). Dextran standards (20, 40, 70, 2000 kDa) and D-galactose were used to calibrate the column. DMSO was used as eluent. Content of AG and its propargyl, triazolyl derivatives in fractions was determined by phenol–sulfuric acid method (Dubois, Gilles, Hamilton, Rebers, & Smith, 1956).

2.3. General procedure for synthesis of AG triazolo derivatives (samples **1**–**8**)

To a stirred solution of propargyl AG (DS 2.0–2.2, 0.19–0.20 g, 1.7 mmol of C≡CH) in DMSO (2.0 mL) the following reagents were added: organyl halide, sodium azide (1:1, see Tables 1 and 2), freshly prepared solution of sodium ascorbate (0.04 g, 0.18 mmol, 11 mol% per C≡CH) in 0.1 mL H_2O, solution of copper(II) sulfate pentahydrate (0.01 g, 0.05 mmol, 3 mol% per C≡CH) in 0.1 mL H_2O and Et_3N (see Tables 1 and 2). After stirring at r.t. the mixture for 6–48 h (see Tables 1 and 2), it was precipitated in 100 mL ethanol. The product was filtered, sequentially washed with water, and ethanol then dried under vacuum.

Some experiments were carried out at 62–65 °C (according to Table 1).

To remove the copper-catalyst, the product (0.4 g) was washed with 5% solution of sodium diethyldithiocarbamate trihydrate in ethanol (100 mL) until the washing water was colorless, then dried under vacuum.

According to second protocol of copper ions removal, the product (0.2 g), dissolved in DMSO (2 mL), was added to cation-exchange resin Dowex 50WX8-200 (0.2 g) and the reaction mixture was stirred for 24 h. Cationite was filtered off and the solution was precipitated in 100 mL ethanol, filtered, sequentially washed with water, and ethanol then dried under vacuum.

The products (carefully washed from the catalyst) are light-yellow powders, insoluble in water and conventional organic solvents, soluble in DMSO, DMF, N-methyl-2-pyrrolidone.

When chloracetic acid was used in cycloaddition reaction, the product was precipitated in 100 mL ethanol, filtered, washed with ethanol and dried under vacuum.

When allylbromide was used in cycloaddition reaction, the product was precipitated in 100 mL water, filtered, washed with water and dried under vacuum.

DS, conversion of C≡CH groups into triazolo derivatives was calculated from EA, quantitative ^{13}C NMR spectroscopy (Tables 1 and 2).

Table 2
Conditions and results of 1,3 dipolar cycloaddition organyc azides (RHal + NaN_3) to arabinogalactan propargyl ethers (DS 2.0–2.2, 1.7 mmol of C≡CH).

Reagents, mmol			Time, h	Conversion of C≡CH[a],%	Products			
RHal	RN_3 (RHal + NaN_3 = 1:1)	Et_3N			Sample	DS		Yield, %
						(EA)[a]	(NMR)[b]	
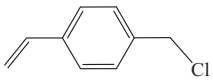	2.7	1.7	12	90	**2**	1.8	–	82
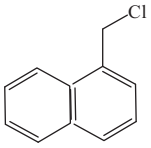	2.7	1.7	12	90	**3**	1.9	2.0	93
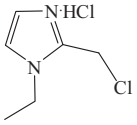	2.7	4.4	12	90	**4**	1.9	2.0	90
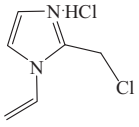	2.7	4.4	12	95	**5**	1.9	1.9	94
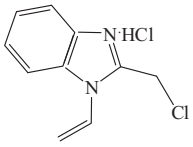	2.7	4.4	12	100	**6**	2.0	2.0	93
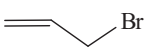	2.7	1.7	12	90	**7**	2.0	1.9	88
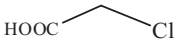	3.4	5.2	48	60	**8**	1.3	–	85

[a] Conversion, DS determined by EA.
[b] DS determined by ^{13}C NMR.

*2.3.1. (1-Benzyl-1,2,3-triazol-4-yl)-methyl AG (sample **1f**)*

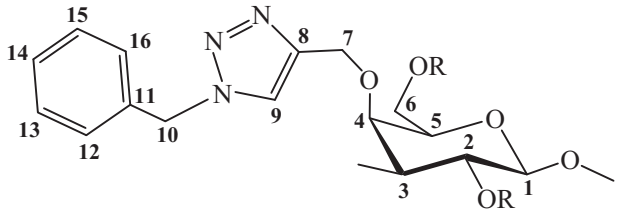

Yield: 0.40 g (93%, taking into account the DS); EA: C 61.00%, H 6.01%, N 16.70%, C/N 3.65; corresponding to DS = 2.1, 100% conversion of C≡CH groups. ^{1}H NMR (δ ppm): 2.9–5.9 (saccharide unit), 4.5 (H-7), 5.4 (H-10), 7.3 (H-12–16), 8.1 (H-9). ^{13}C NMR (δ ppm): 52.9 (C-10), 60.0–66.0 (C-7), 66.0–90.0 (saccharide unit, C-2—C-6), 100.0–110.0 (C-1), 123.9 (C-9), 126.0–130.0 (C-12—C-16), 135.8 (C-11), 144.1, 144.8 (C-8); estimated DS = 2.0. IR (cm^{-1}): 3430 (O—H), 3136 (C—H, triazole), 3089, 3064, 3032 (C—H, phenyl), 2932, 2874 (C—H), 1606, 1587, 1497, 1455 (C=C, phenyl), 1125, 1092, 1048 (C—O).

*2.3.2. (1-[4-Vinylbenzyl]-1,2,3-triazol-4-yl)-methyl AG (sample **2**)*

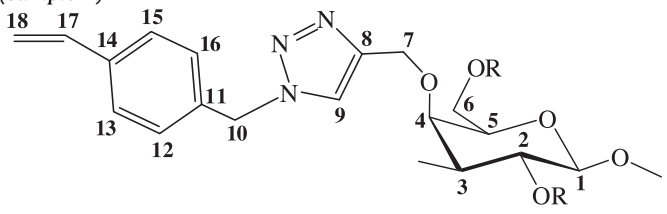

Yield: 0.36 g (82%, taking into account the DS); EA: C 64.25%, H 5.75%, N 14.28%, C/N 4.50; corresponding to DS = 1.8, 90% conversion of C≡CH groups. ^{1}H NMR (δ ppm): 2.9–5.9 (saccharide unit), 4.6 (H-7), 5.2 (H-10), 5.4–6.4 (CH=CH$_2$, H-17, H-18), 6.7–7.9 (H-12, H-13, H-15, H-16), 8.1 (H-9). ^{13}C NMR (δ ppm): 52.4 (C-10), 60.0–66.0 (C-7), 66.0–90.0 (saccharide unit, C-2—C-6), 100.0–110.0 (C-1), 114.6 (C-18), 123.8 (C-9), 125.0–130.0 (C-12, C-13, C-15, C-16), 135.3 (C-11), 135.9 (C-14), 136.8 (C-17), 144.0, 144.7 (C-8). IR (cm^{-1}): 3430 (O—H), 3135 (C—H, triazole), 3086, 3061, 3024 (C—H, Ar), 3008 (C—H, CH=CH$_2$) 2926, 2874 (C—H), 1629 (C=C, CH=CH$_2$), 1612, 1569, 1513 (C=C, Ar), 1125, 1092, 1048 (C—O).

*2.3.3. (1-[1-Naphthylmethyl]-1,2,3-triazol-4-yl)-methyl AG (sample **3**)*

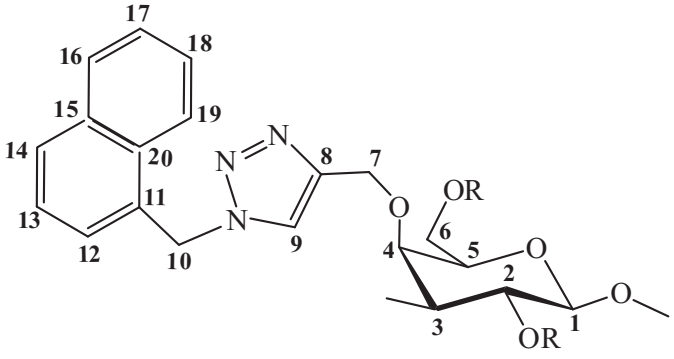

Yield: 0.46 g (93%, taking into account the DS); EA: C 65.45%, H 5.54%, N 13.24%, C/N 4.94; corresponding to DS = 1.9, 90% conversion of C≡CH groups. ^{1}H NMR (δ ppm): 2.9–5.9 (saccharide unit), 4.4 (H-7), 5.9 (H-10), 6.7–8.2 (H-9, H-12—H-14, H-16—H-19). ^{13}C NMR (δ ppm): 52.4 (C-10), 60.0–66.0 (C-7), 66.0–90.0 (saccharide unit, C-2—C-6), 100.0–110.0 (C-1), 114.6 (C-15), 123.8 (C-9), 125.0–129.0 (C-12—C-14, C-16, C-18, C-19), 135.3 (C-17), 135.9 (C-20), 136.8 (C-11), 143.9, 144.6 (C-8); estimated DS = 2.0. IR (cm^{-1}): 3436 (O—H), 3140 (C—H, triazole), 3061, 3014 (C—H, naphthyl), 2926, 2875 (C—H), 1599, 1512 (C=C, naphthyl), 1117, 1091, 1048 (C—O).

*2.3.4. (1-[(1-Ethylimidazol-2-yl)methyl]-1,2,3-triazol-4-yl)-methyl AG (sample **4**)*

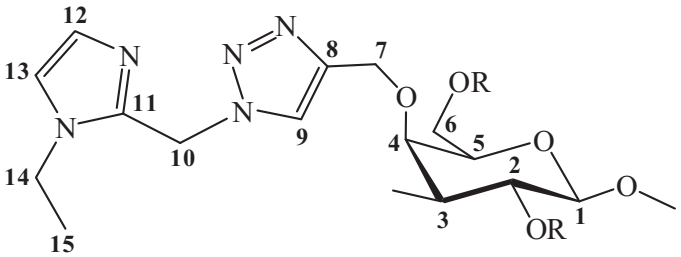

Yield: 0.40 g (90%, taking into account the DS); EA: C 52.42%, H 5.66%, N 24.67%, C/N, 2.12; corresponding to DS = 1.9, 90% conversion of C≡CH groups. ^{1}H NMR (δ ppm): 1.1 (H-15), 2.9–5.9 (saccharide unit), 4.0 (H-14), 4.5 (H-7), 5.7 (H-10), 6.8 (H-12), 7.2 (H-13), 8.0 (H-9). ^{13}C NMR (δ ppm): 15.9 (C-15), 40.6 (C-14, DMSO-d$_6$), 45.0 (C-10), 60.0–66.0 (C-7), 66.0–90.0 (saccharide unit, C-2—C-6), 100.0–110.0 (C-1), 120.6 (C-13), 124.0 (C-9), 127.5 (C-12), 140.8 (C-11), 144.0, 144.9 (C-8); estimated DS = 2.0. IR (cm^{-1}): 3420 (O—H), 3136 (C—H, triazole), 3110 (C—H, imidazole), 2980, 2937, 2879 (C—H), 1494, 1467 (C=C, imidazole), 1140, 1091, 1048 (C—O).

*2.3.5. (1-[(1-Vinylimidazol-2-yl)methyl]-1,2,3-triazol-4-yl)-methyl AG (sample **5**)*

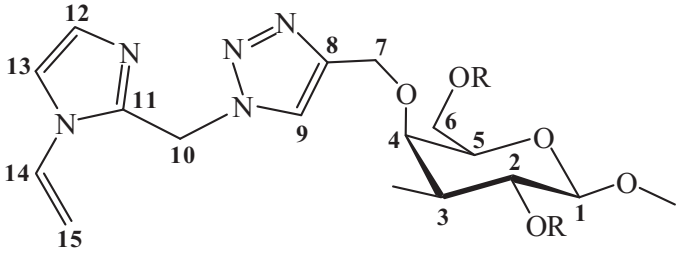

Yield: 0.42 g (94%, taking into account the DS); EA: C 52.56%, H 5.34%, N 25.02%, C/N 2.10; corresponding to DS = 1.9, 95% conversion of C≡CH groups. ^{1}H NMR (δ ppm): 2.9–5.9 (saccharide unit), 4.4 (H-7), 4.9 (H-15), 5.4 (H-15), 5.8 (H-10), 6.9 (H-12), 7.3 (H-14), 7.6 (H-13), 8.0 (H-9) ^{13}C NMR (δ ppm): 45.26 (C-10), 60.0–66.0 (C-7), 66.0–90.0 (saccharide unit, C-2—C-6), 100.0–110.0 (C-1, C-15), 117.7 (C-13), 124.5 (C-9), 129.0 (C-12; C-14), 141.4 (C-11), 144.3, 145.2 (C-8); estimated DS = 1.9. IR (cm^{-1}): 3420 (O—H), 3136 (C—H, triazole), 3110 (C—H, imidazole), 3003 (C—H, CH=CH$_2$), 2966, 2920, 2875 (C—H), 1646 (C=C, CH=CH$_2$), 1526, 1487 (C=C, imidazole), 1135, 1089, 1048 (C—O).

*2.3.6. (1-[(1-Vinylbenzimidazol-2-yl)methyl]-1,2,3-triazol-4-yl)-methyl AG (sample **6**)*

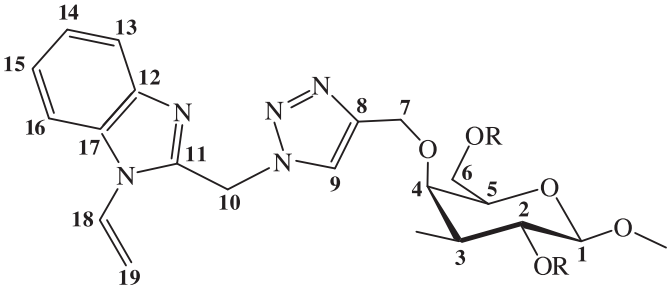

Yield: 0.49 g (93%, taking into account the DS); EA: C 60.18%, H 5.00%, N 21.96%, C/N 2.74; corresponding to DS = 2.0, 100% conversion of C≡CH groups. ^{1}H NMR (δ ppm): 2.9–5.9 (saccharide unit), 4.6 (H-7), 5.0–6.5 (H-19, H-10), 6.5–7.9 (H-13—H-16, H-18), 8.2 (H-9). ^{13}C NMR (δ ppm): 46.2 (C-10), 60.0–66.0 (C-7), 66.0–90.0 (saccharide unit, C-2—C-6), 100.0–110.0 (C-1, C-19), 111.7 (C-16), 119.5 (C-13), 122.9 (C-15), 123.8 (C-14), 124.5 (C-9), 128.3 (C-18), 133.5 (C-17), 142.0 (C-12), 143.9, 144.9 (C-8), 147.9 (C-11); estimated DS = 2.0. IR (cm^{-1}): 3430 (O—H), 3138 (C—H, triazole), 3089, 3057 (C—H, benzimidazole), 3002 (C—H, CH=CH$_2$), 2922, 2875 (C—H), 1645 (C=C, CH=CH$_2$), 1611, 1524, 1458 (C=C, benzimidazole), 1161, 1087, 1047 (C—O).

2.3.7. (1-Allyl-1,2,3-triazol-4-yl)-methyl AG (sample **7**)

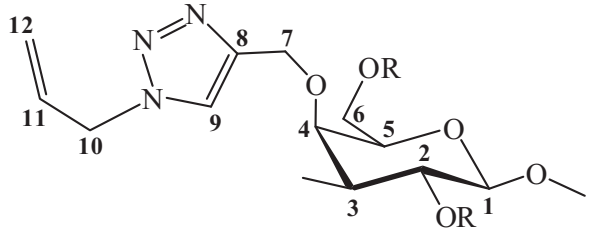

Yield: 0.30 g (88%, taking into account the DS); EA: C 51.79%, H 6.51%, N 19.42%, C/N 2.67; corresponding to DS = 2.0, 90% conversion of C≡CH groups. ^{1}H NMR (δ ppm): 2.9–5.9 (saccharide unit), 4.0–5.5 (H-7, H-10, H-12) 6.0 (H-11), 8.0 (H-9). ^{13}C NMR (δ ppm): 52.2 (C-10), 60.0–66.0 (C-7), 66.0–90.0 (saccharide unit, C-2—C-6), 100.0–110.0 (C-1), 118.7 (C-12), 123.8 (C-9), 133.4 (C-11), 143.8, 144.6 (C-8); estimated DS = 1.9. IR (cm^{-1}): 3434 (O—H), 3138 (C—H, triazole), 3087, 3020 (C—H, CH=CH$_2$), 2980, 2926, 2877 (C—H), 1645 (C=C, CH=CH$_2$), 1143, 1093, 1049 (C—O).

2.3.8. (Sodium carboxymethyl-1,2,3-triazol-4-yl)-methyl AG (sample ***8***)

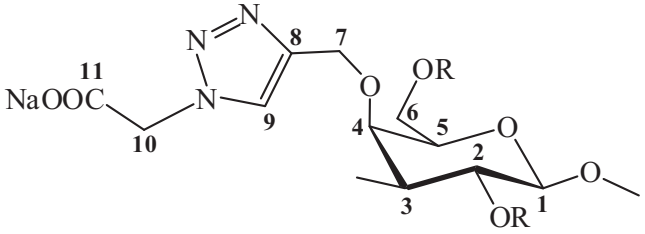

Yield: 0.28 g (85%, taking into account the DS); EA: C 42.75%, H 6.01%, N 13.46%, ash 9.90%; Na 6.29%, Cu 1.53%, C/N 3.18; corresponding to DS = 1.3, 60% conversion of C≡CH groups. ^{1}H NMR (δ ppm): 2.9–5.9 (saccharide unit), 4.6 (H-7), 5.3 (H-10), 8.1 (H-9). ^{13}C NMR (δ ppm): 50.7 (C-10), 54.0–90.0 (saccharide unit, C-2—C-6, and C-7), 100.0–110.0 (C-1), 124.9 (C-9), 144.4 (C-8), 168.6 (C-11). IR (cm^{-1}): 3435 (O—H), 3290 (C—H, C≡CH), 3137 (C—H, triazole), 2930, 2884 (C—H), 2118 (C≡C), 1626, 1392 (COO$^-$), 1140, 1094, 1061 (C—O).

3. Results and discussion

In all the experiments, propargylated AG with DS 2.0–2.2, soluble in a number of organic solvents (Grischenko et al., 2013), has been used as the starting material for the synthesis of triazolo derivatives of AG via CuAAC. Organic azide is generated in situ from alkyl halide and sodium azide that allows preliminary stages of its preparation and isolation to be excluded. CuAAC reaction is carried out at room temperature or slight heating (62–65 °C) in the mixture DMSO/water (10:1) in the presence of traditional Sharpless-Fokin catalytic system: copper(II) sulfate plus sodium ascorbate as reducing agent required to maintain copper in the active oxidation state [Cu(I)].

The choice of DMSO-water mixture as medium is defined, first of all, by its good dissolving ability toward both propargylated AG and salts of the catalytic system. Besides, it is known that copper ions promote the generation of reactive oxygen species (e.g. •OH, $O_2^{\bullet -}$) under CuAAC conditions, which can cause depolymerization of different polysaccharides (Elchinger et al., 2011; Fry, 1998; Lallana et al., 2011; Lallana, Sousa-Herves, Fernandez-Trillo, Riguera, & Fernandez-Megia, 2012; Nakagawa et al., 2012), whereas DMSO is a classical radical scavenger (Fry, 1998).

The removal of Cu ions from products is difficult and is attained by multiple washing of the products with ethanol solution of sodium diethyldithiocarbamate (a very efficient complexing agent) or by one-day treatment of their solution in DMSO with cation-exchange resin Dowex 50WX8-200.

The conditions of AG triazolo derivatives synthesis have been optimized using the cycloaddition of AG propargyl ethers with benzyl chloride and sodium azide, the most simple and well studied compounds in the CuAAC (Scheme 1, R = Bn; Table 1).

It is assumed that the addition of amines significantly accelerates the CuAAC reaction only if Cu(I)-halide salts are employed as the catalysts, while the catalytically active Cu(I) species are directly generated by reduction with ascorbate and immediately form the corresponding Cu-acetylides (Berg & Straub, 2013; Meldal, 2008). Indeed, in some of the above-cited works (Elchinger et al., 2012; Eyley & Thielemans, 2011; Koschella et al., 2010; Liebert, Hänsch, & Heinze, 2006; Oliveira, Martins, Mafra, & Gomes, 2012; Tahir, Lämmerhardt, & Mischnick, 2012), amines are not used in the synthesis of polysaccharide triazolo derivatives, but our experiments have shown that in the presence of Et_3N, triazoles are formed noticeably faster. For example, without Et_3N for 12 h, only 10% of AG propargyl groups participate in the reaction (Table 1, sample **1b**), while the addition of Et_3N for same time (0.3–1.0 eqv. per AG triple bonds) increase their conversion to 80% (Table 1, sample **1c**).

By varying the reaction conditions, we have achieved complete conversion of AG propargyl groups, AG triazolo derivatives being formed in high yields. It turns out that the reaction is effective already at room temperature and equimolar ratio of BnCl:NaN_3:C≡CH (Table 1, sample **1c**), however the process rate considerably increases when the reagents, forming organic azide, are used in small excess. For example, if the ratio of BnCl:NaN_3:C≡CH is 1.6:1.6:1, the conversion of the AG propargyl groups augments for 6 h from 59 to 90% (Table 1, cf. samples **1a** and **1e**), while total conversion is attained for 12 h (Table 1, sample **1f**). The raise of temperature (from r.t. to 62–65 °C) expectedly accelerates the process (Table 1, cf. sample **1a** and **1d**), but the heating in open system (with the reflux condenser) is accompanied by intensive brown coloring of the reaction mixture thus evidencing the disproportionation of Cu(I) to Cu(0) and Cu(II) and the re-oxidation to Cu(II) by air (Fry, 1998; Meldal, 2008), i.e. the catalyst decomposition takes place. Besides, these experiments are less reproducible (Table 1, cf. conversion in samples **1g** and **1h**).

In the IR spectra of the products, absorption bands of the terminal alkynes considerably reduce or completely disappear (3290, 2117 cm^{-1}), while absorption bands of the triazole (3136 cm^{-1}) and phenyl (3090, 3065, 3030, 1606, 1497, 1455 cm^{-1}) groups are observed.

In the ^{1}H, ^{13}C NMR spectra, signals of all structural units of AG benzyltriazolo derivatives (samples **1a**–**h**) are detected (Figs. 1 and 2). For comparison is also shown the ^{13}C NMR spectrum of starting propargylated AG.

DS of the AG triazolo derivatives can be calculated from N-content (determined by elemental analysis (EA)) and on the basis of quantitative ^{13}C NMR by the equation 1. The latter defines the ratio

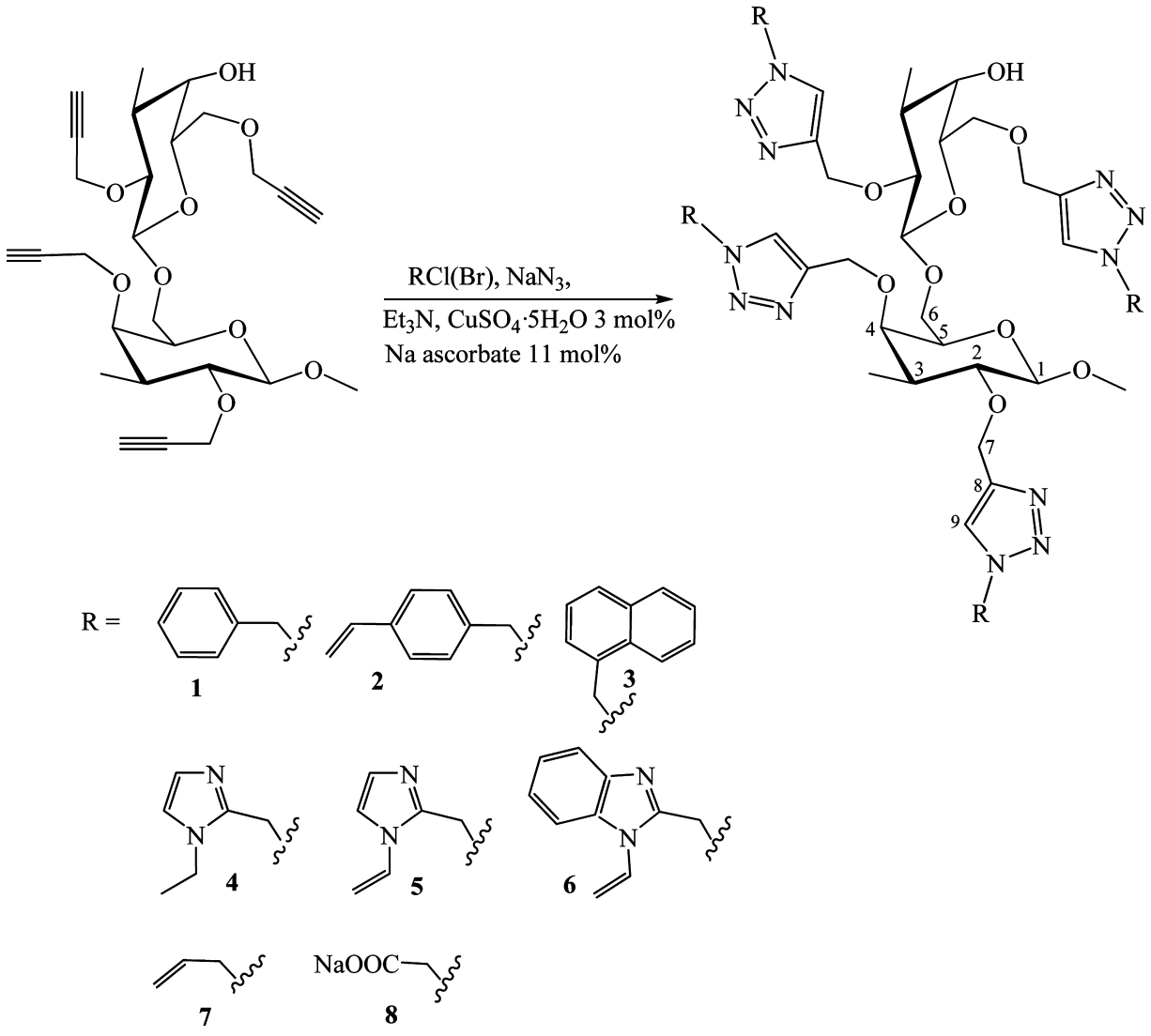

Scheme 1. Synthesis of 1,4-disubstituted 1,2,3-triazole derivatives of AG.

of signal intensity of the C-8 triazole carbon (144 ppm) to signal intensity of the AG anomeric carbon C-1 (100–110 ppm):

$$DS = \frac{\int C^8}{\int C^1} \quad (1)$$

where $\int C^8$ is integral of triazole quaternary carbon at 144 ppm; $\int C^1$ is integral of anomeric carbon at 100–110 ppm.

DS of the products is defined by conversion the propargyl groups of the initial AG to triazoles. At 100% conversion, DS of the products is equal to DS of the starting propargyl AG (2.0–2.2). For instance, DS of sample **1f** (Table 1), calculated by the equation 1, is 2.0. The data of EA (% N = 16.70, C = 61.00, C:N = 3.65, Supplementary data), which has been used in most cases, give the same value (DS = 2.1). Since the starting propargyl ether has the same DS value, one can assume that it is completely converted into the corresponding AG triazolo derivative. This assumption is confirmed by the IR spectrum of sample **1f** where absorption bands of the propargyl groups are absent.

The weight-average molecular mass of the product (Table 1, sample **1f**), determined by gel permeation chromatography (GPC) (15 kDa, Fig. 3) is lower than that of both the initial AG propargyl ether (18 kDa) and AG (16 kDa), although the molar mass of the modified repeating units increases after CuAAC reaction. It indicates the depolymerization of AG polysacharide backbone. As it has been already mentioned, such depolymerization is likely due to the destructive action of reactive oxygen species, which are known (Elchinger et al., 2011; Fry, 1998; Hong, Presolski, Ma, & Finn, 2009; Kulbokaite, Ciuta, Netopilik, & Makuska, 2009; Lallana, Fernandez-Megia, & Riguera, 2009; Lallana et al., 2011, 2012) to be formed under the conditions of CuAAC of reaction from oxygen air in the presence copper(II)/ascorbate system. Interestingly, it is reported (Miller, 1986) that in the absence of metals, AG undergoes depolymerization under the action of hydrogen peroxide to a lesser extent than other polysaccharides.

The conditions developed for CuAAC of propargylated AG with sodium azide and benzyl chloride have been successfully applied to the reactions of AG propargyl ethers (Scheme 1) with sodium azide and such organyl halides as chloromethylarenes (Table 2, samples **2** and **3**), chloromethylimidazoles (in the form of salts with HCl, Table 2, samples **4**–**6**), allyl bromide (Table 2, sample **7**), and chloroacetic acid (Table 2, sample **8**).

According to the IR and NMR data, among the reaction products, noticeable amounts of unreacted propargyl groups are detected only in the case when chloroacetic acid is used. In other cases, the conversion of the propargyl moiety is complete or close to 100%. In the IR spectra of the products, absorption bands significantly decrease or disappear at 3290 and 2117 cm^{-1}, in the NMR spectra

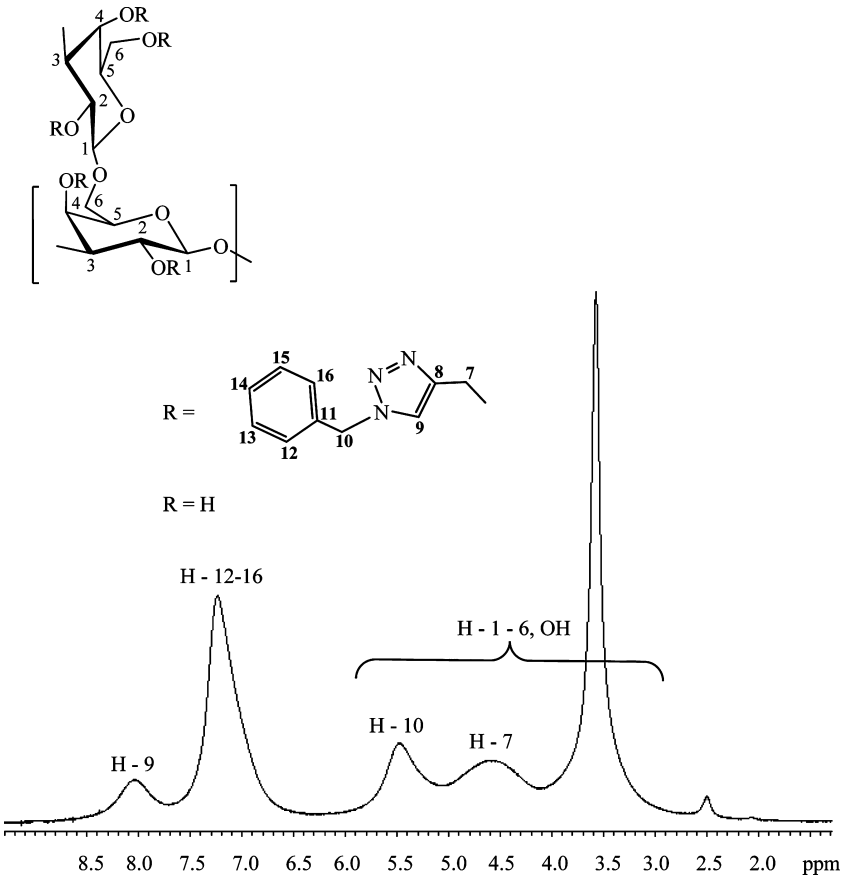

Fig. 1. ^{1}H NMR spectrum of (1-benzyl-1,2,3-triazol-4-yl)-methyl AG (sample **1f**).

(DMSO-d_6), the signals of carbon atoms decrease at 76–79 and 80–83 ppm that is typical for monosubstituted alkynes.

At the same time, in the IR and NMR spectra, absorption bands and the signals caused by the formation of triazole cycles and introduction of the corresponding substituents (Ar, imidazole, allyl, carboxyl) appear (Supplementary data). For example, the absorption bands at 3110–3030 cm^{-1} and 1610–1400 cm^{-1} can be assigned to vibrations of the aromatic and heteroaromatic moieties. The triazole group is evidenced by a weak band at 3140–3135 cm^{-1}. The IR spectra of compounds **2**, **5**, **6** and **7** show a strong absorption band of the vinyl group C=C bond at 1646–1629 cm^{-1} and a weak band of =C–H bond in the region 3090–3000 cm^{-1}, while a strong band at 1626 cm^{-1} corresponds to the carbonyl group (sample **8**). In the NMR spectra (DMSO-d_6), the triazole proton resonance appears at 8.0–8.2 ppm, the characteristic signals of the triazole carbon atoms are detected at 124 and 144 ppm, the C atoms of the NCH_2 and OCH_2 moieties give peaks at 45.0–52.4 ppm and 63.5–65.4 ppm, respectively. The signals in the region 66.0–90.0 and 100–110 ppm are attributed to the carbons of the AG repeating saccharide unit. The peaks of the aromatic carbon atoms (samples **2**, **3**, **6**) can be observed between 111.7 and 142.0 ppm. The characteristic signals of the imidazole carbon atoms (samples **4**–**6**) present at 117.7–133.5, 127.5–142.0 and 140.8–147.9 ppm. The resonance of the vinyl moiety in samples **2** and **7** ($\underline{C}H_2=\underline{C}H-C$) occur in the regions 114.6–118.7 ($CH_2=$) and 133.4–136.8 ppm (=CH) and for carbon atoms of the vinyl moiety in samples **5** and **6** ($CH_2=CH-N$) at 103.5–108.0 ($CH_2=$) and 128.3–129.0 ppm (=CH). Signals of the ethyl group in 1-ethylimidazole substituent (sample **4**) present at 15.9 and 40.6 ppm, the latter is overlapped with signal of the solvent (DMSO-d_6 δ_C = 39.5). The peak of the carbon atom of the carbonyl function (sample **8**) resonates at 168.6 ppm.

DS of AG triazolo derivatives can be calculated from N content (determined by EA) as well as on the basis of quantitative ^{13}C NMR spectra (Table 2, samples **2**–**8**). In the latter case, DS of majority of the products (Table 2, samples **2**, **3**, **4**, **7**) are calculated by the equation 1. The exceptions are samples **5** and **6** (Table 2) containing the vinylimidazole fragment. In the ^{13}C NMR spectra (DMSO-d_6) (Fig. 4) of these compounds, signals of the vinyl group ($CH=CH_2$) carbons are observed at 128–129 and 103–108 ppm and overlapped with signals of the imidazole cycle (117–120, 127–142, 140–147 ppm) and anomeric C-1 carbon atom (100–110 ppm). Therefore for DS calculation in these samples, the Eq. (2) is used:

$$DS = \frac{5 \cdot \int C^{8}}{\int C^{2-6} + C^{7} - \int C^{8}} \quad (2)$$

where $\int C^{8}$ is integral of the triazole quaternary carbon; $\int C^{2-6} + C^{7}$ is summarized integral of five carbons in galactose unit and carbon of the OCH_2 group bonded with the triazole ring (at 60–90 ppm).

The DS values calculated by both methods, practically coincide (Table 2) and along with spectral data testify to very high or full conversion of the AG propargyl groups in triazoles (in 82–94% yields).

As mentioned above, the only exception is the product formed by treatment of propargyl AG with chloroacetic acid and sodium azide (Table 2, sample **8**). Despite the high concentration of organic azide in the reaction mixture (a band at 2103 cm^{-1}), the maximum conversion of AG propargyl groups is only 60%, probably due to the reaction of sodium azide with acidic functions of chloroacetic acids. DS calculated by EA (C/N ratio 3.18) is 1.3. In the IR spectrum of carboxytriazolo AG (sample **8**), the absorption bands of residual triple bonds are detected at 3290 and 2118 cm^{-1}, and the

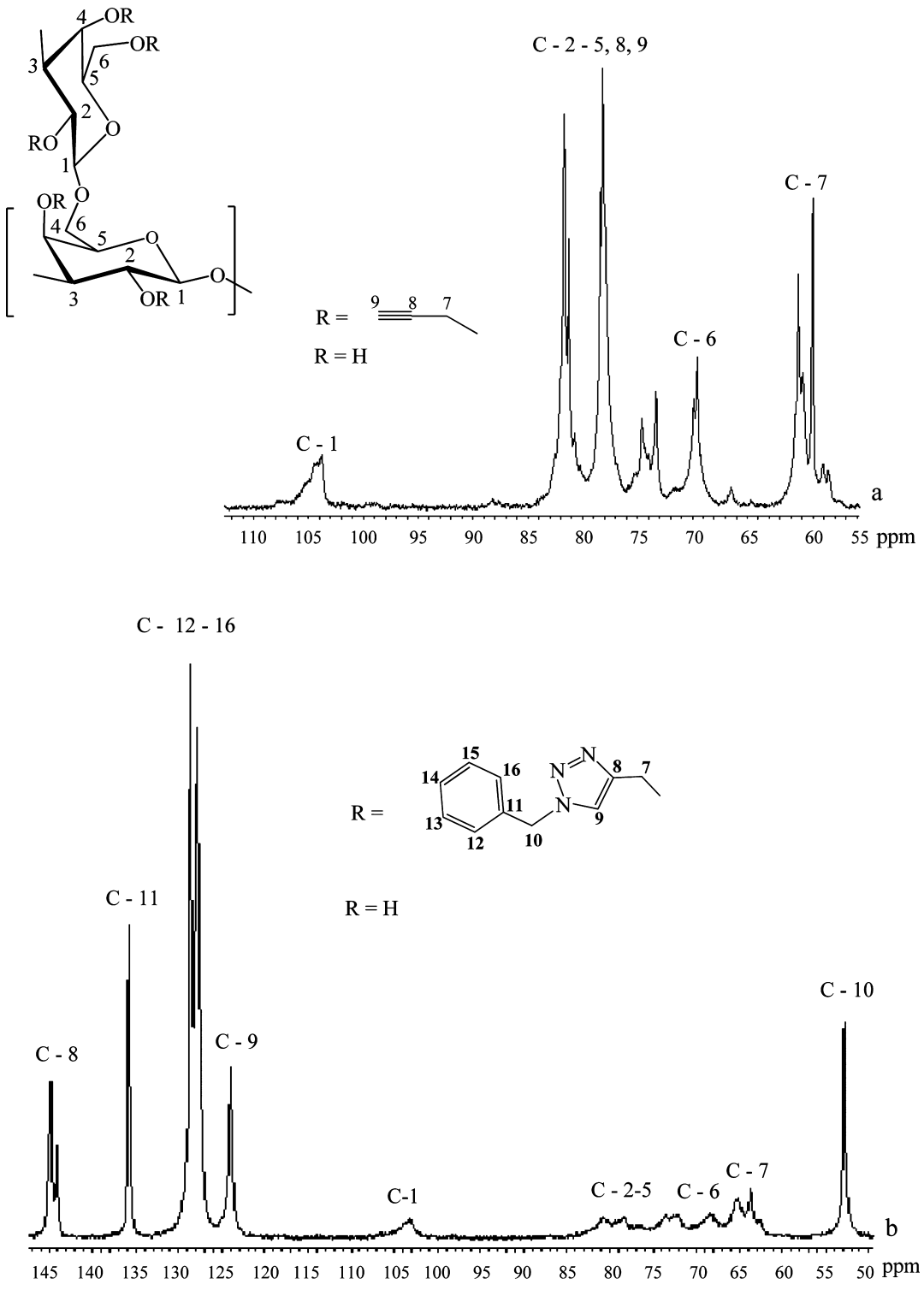

Fig. 2. ^{13}C NMR spectra of starting propargylated (a) and (1-benzyl- 1,2,3-triazol-4-yl)-methyl (b) (sample **1f**) AG.

absorption band of carboxylate anion is observed at 1626 cm^{-1}. Besides, sample **8** contains 6.3% of sodium (EA data) that indicates that this sample has been prepared in the form of sodium salt. Since the salt is not dissolved in DMSO, slowdown of the reaction is probably due to the decrease of AG derivatives solubility in the course of introduction into their structure of the carboxyl groups.

Despite formation of the salt, sample **8** is poorly soluble in water to give viscous gels. After treatment with 1 N HCl, water-solubility is completely lost, however it becomes possible to obtain DMSO solutions of low concentration and record the NMR spectra. In the ^{13}C NMR spectrum (DMSO-d_6) (Fig. 5), a broad signal at 56–60 ppm confirms the existence of remaining CH_2 carbon atoms of the propargyl moieties. Attempts to obtain quantitative ^{13}C NMR spectrum of sample failed due to low concentration and high viscosity of solutions.

In the majority of the samples, no residual amounts of copper are detected, with a precision of ±0.05% in accordance with the used energy-dispersive X-ray microanalyses method. The exception is the sample **8** (1.53% Cu), which was not additionally purified.

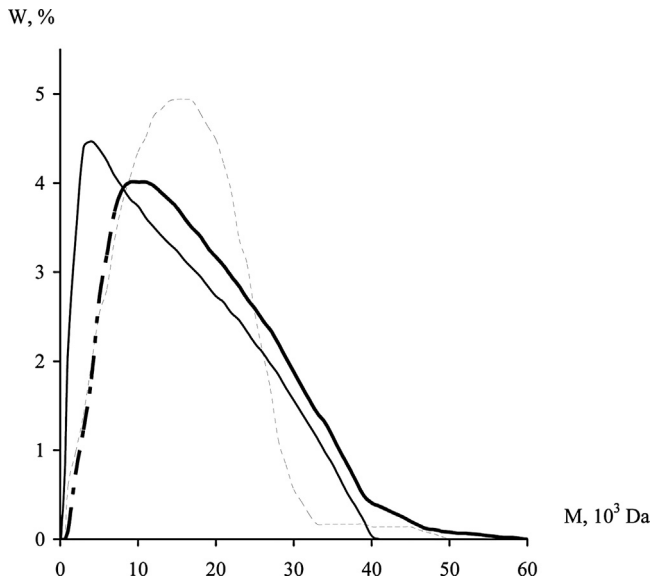

Fig. 3. GPC of (1-benzyl-1,2,3-triazol-4-yl)-methyl AG (sample **1f**, —), AG propargyl ether (▬), AG (- - -). W – relative amount of polysaccharide.

Depending upon the introduced function, triazolo AGs show different solubility. All of them (apart from the aforementioned sodium carboxymethyltriazoles) are well soluble in DMSO, DMF and insoluble in water. The allyltriazolo AG (sample **7**) is soluble in ethanol and acetone, whereas triazolo AG containing a 1-ethylimidazole fragment (sample **4**) is soluble in a mixture of ethanol and acetone.

Thus, the application of CuAAC has allowed us to implement a one-stage synthesis of molecular ensembles combining natural biologically active polysaccharide AG with 1,2,3-triazoles and imidazoles, which found extensive application in organic, bioorganic and medicinal chemistry. Such modifications of AG are promising building blocks for drug design and can be used also for preparation of plant protection products and plant growth regulators.

The triazolo AG (sample **5**) has exhibited the excellent coordination ability toward Fe(III), Cu(II), Co(II), Zn(II) ions. The complexes formed have included up to the three of imidazole moieties per one metal ion. Noteworthy, in comparison with the initial water insoluble ligand, its complexes with Fe(III) and Cu(II) ions have been water soluble, that is substantial for their biocompatibility.

As an example, the quaternization of 1,2,3-triazolo AGs–(1-benzyl-1,2,3-triazol-4-yl)-methyl AGs with methyl iodide has led to triazolium cations, potentially active centers for conjugation of DNA and RNA, oligonucleotide molecules, that has lighten their further transportation.

Some of the synthesized compounds contain reactive unsaturated groups that makes it possible their further modifications for the purpose of creation of environmentally benign materials. Sodium carboxytriazolo AG can be exploited as new water soluble polyelectrolyte.

Investigations concerning the stability and the biological activity of the triazoles, binding of large bioactive AG molecule are under progress.

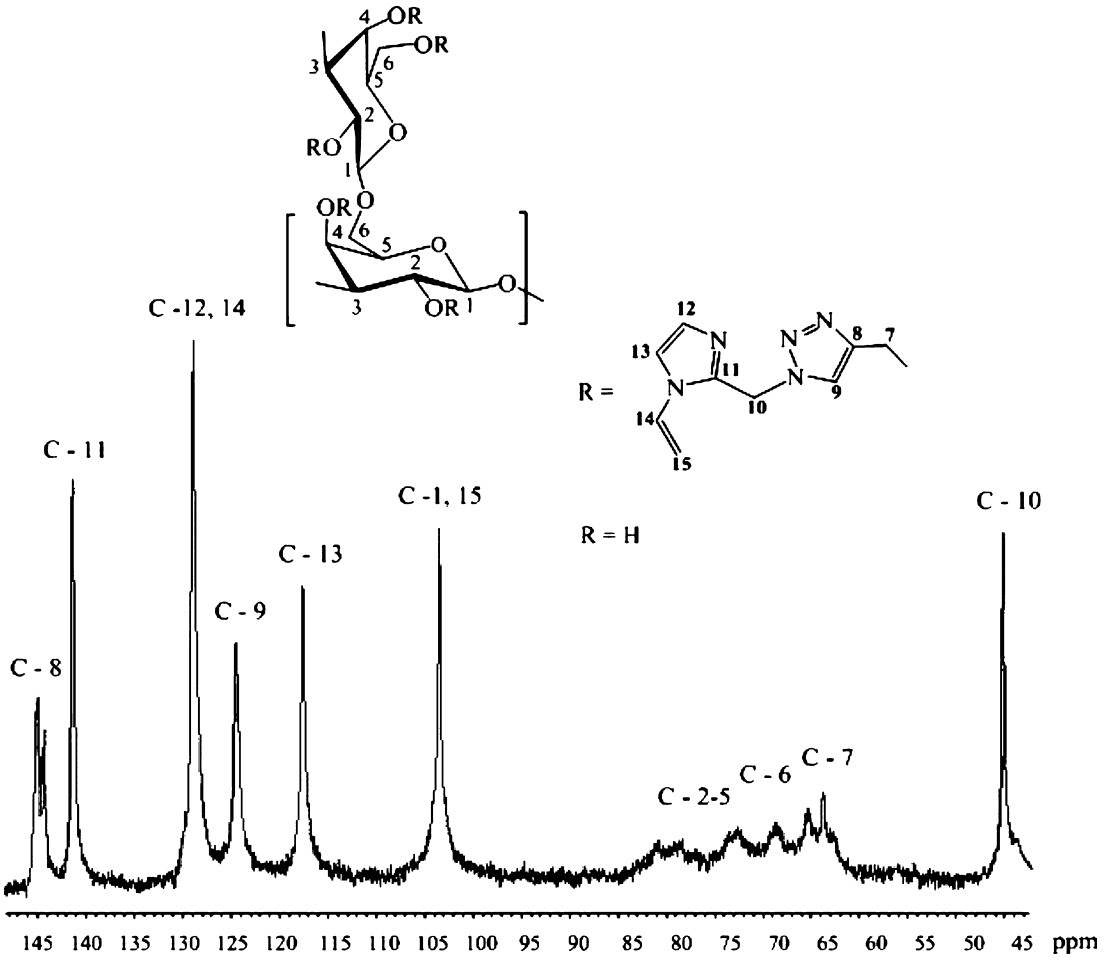

Fig. 4. ^{13}C NMR spectrum of (1-[(1-vinyl-imidazol-2-yl)methyl]-1,2,3-triazol-4-yl)-methyl AG (sample **5**).

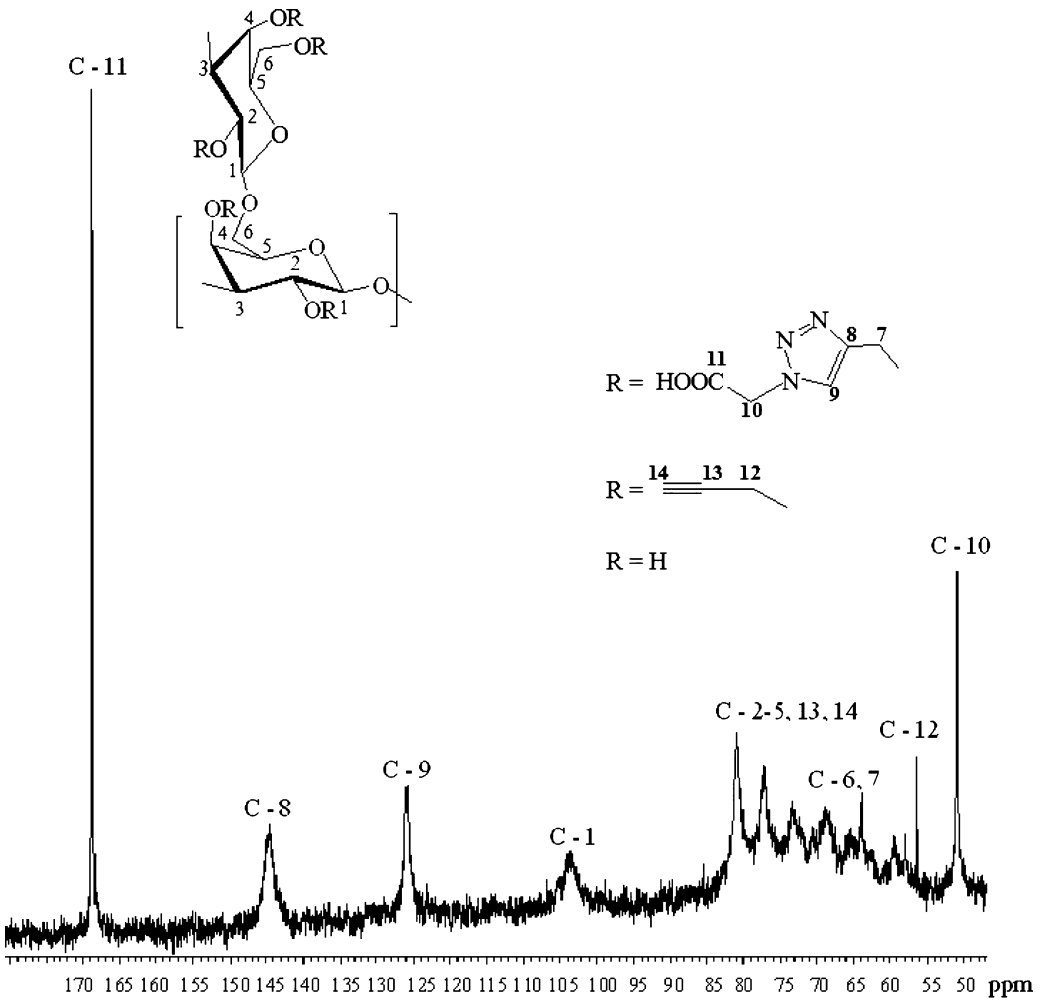

Fig. 5. ^{13}C NMR spectrum of (carboxymethyl-1,2,3-triazol-4-yl)-methyl AG (sample **8**).

4. Conclusion

The copper-catalyzed reaction of the AG propargyl ethers with sodium azide and organyl halides leads to a variety selectively functionalized AG triazolo derivatives including benzyl, vinylbenzyl, naphthylmethyl, vinylimidazolylmethyl, ethylimidazolylmethyl, vinylbenzimidazolylmethyl, allyl, and carboxymethyl substituents. Conversion of terminal alkyne groups is complete or close to 100%. EA, IR, ^{1}H NMR and ^{13}C NMR spectra support the structural uniformity of the synthesized AG derivatives. Introduction of the desired functional modules with triazole linker into AG could be useful for designing novel AG materials with specific properties depending on the functional groups that increases their potential for versatile applications.

Appendix A. Supplementary data

Supplementary data associated with this article can be found, in the online version, at http://dx.doi.org/10.1016/j.carbpol.2014.08.050.

References

Aleksandrova, G. P., Grishchenko, L. A., Bogomyakov, A. S., Sukhov, B. G., Ovcharenko, V. I., & Trofimov, B. A. (2010). Magnetic activity of nanostructured biopolymeric nanomagnets. *Russian Chemical Bulletin International Edition*, *59*, 2318–2322.

Babkin, V. A., Ivanova, S. Z., Fedorova, T. E., Medvedeva, E. N., Malkov, Yu. A., Ostroukhova, L. A., et al. (2007). Scientific basis of technology of complex processing of larch biomass. *Khimiya Rastitelnogo Syrya*, 9–21, *Chemical Abstracts, 151*, 315978 (2008)

Babkin, V. A., Kolzunova, L. G., Medvedeva, E. N., Malkov, Yu. A., & Ostroukhova, L. A. (2005). *Method for production of arabinogalactan*. R.F. Patent 2 256 668; *Chemical Abstracts, 143*, 117081.

Baikalova, L. V., Domnina, E. S., & Skvortsova, G. G. (1977). Izvestiya Akademii Nauk SSSR. *Seriya Khimicheskaya*, *5*, 1158–1161, *Chemical Abstracts 87*, 84894b.

Berg, R., & Straub, B. F. (2013). Advancements in the mechanistic understanding of the copper-catalyzed azide–alkyne cycloaddition. *Beilstein Journal of Organic Chemistry*, *9*, 2715–2750.

Corot, C., Robert, P., Idée, J.-M., & Port, M. (2006). Recent advances in iron oxide nanocrystal technology for medical imaging. *Advanced Drug Delivery Reviews*, *58*, 1471–1504.

D'Adamo, P. (1990). Larch arabinogalactan. *Journal of Naturopathic Medicine*, *6*, 33–37.

Dubois, M., Gilles, K. A., Hamilton, J. K., Rebers, P. A., & Smith, F. (1956). *Analytical Chemistry*, *28*, 350–356.

Dubrovina, V. I., Medvedeva, S. A., Aleksandrova, G. P., Tukavkina, N. A., Golubinsky, E. P., IvanovaF S.Z., et al. (2001). Immunomodulating properties of arabinogalactan from *Larix sibirica* L. *Farmatsiya (Moscow)*, *5*, 26–27, *Chemical Abstracts, 137*, 103582.

Elchinger, P.-H., Faugeras, P.-A., Boëns, B., Brouillette, F., Montplaisir, D., Zerrouki, R., et al. (2011). Polysaccharides: The "click" chemistry impact. *Polymers*, *3*, 1607–1651.

Elchinger, P.-H., Montplaisir, D., & Zerrouki, R. (2012). Starch–cellulose crosslinking – Toward a new material. *Carbohydrate Polymers*, *87*, 1886–1890.

Elgart, A., Farber, S., Domb, A. J., Polacheck, I., & Hoffman, A. (2010). Polysaccharide pharmacokinetics: Amphotericin B arabinogalactan conjugate – A drug delivery system or a new pharmaceutical entity? *Biomacromolecules*, *11*, 1972–1977.

Enomoto-Rogers, Y., Kamitakahara, H., Yoshinaga, A., & Takano, T. (2012). Comb-shaped graft copolymers with cellulose side-chains prepared via click chemistry. *Carbohydrate Polymers*, *87*, 2237–2245.

Eyley, S., & Thielemans, W. (2011). Imidazolium grafted cellulose nanocrystals for ion exchange applications. *Chemical Communications*, *47*, 4177–4179.

Fry, S. C. (1998). Oxidative scission of plant cell wall polysaccharides by ascorbate-induced hydroxyl radicals. *Biochemical Journal*, *332*, 507–515.

Gao, Y., Zhang, Z., Chen, L., Gu, W., & Yaping, L. (2009). Synthesis of 6-N,N,N-trimethyltriazole chitosan via "click chemistry" and evaluation for gene delivery. *Biomacromolecules*, *10*, 2175–2182.

Gasilova, E. P., & Aleksandrova, G. P. (2011). Influence of gold content on colloidal structure of gold nanoparticles capped with arabinogalactan. *Journal of Physical Chemistry C*, *115*, 24627–24635.

Gasilova, E. P., Matveeva, G. N., Aleksandrova, G. P., Sukhov, B. G., & Trofimov, B. A. (2013). Colloidal aggregates of Pd nanoparticles supported by larch arabinogalactan. *Journal of Physical Chemistry B*, *117*, 2134–2141.

Gasilova, E. P., Toropova, A. A., Bushin, S. V., Khripunov, A. K., Grishchenko, L. A., & Aleksandrova, G. P. (2010). Light scattering from aqueous solutions of colloid metal nanoparticles stabilized by natural polysaccharide arabinogalactan. *Journal of Physical Chemistry B*, *114*, 4204–4212.

Gendler, T. S., Novakova, A. A., Prudnikov, V. N., Aleksandrova, G. P., & Grishchenko, L. A. (2009). Comparative analysis of γ-Fe_2O_3 nanoparticles magnetic interactions in different polymeric nanocomposites. *Solid State Phenomena*, *152–153*, 269–272.

Grishchenko, L. A., Medvedeva, S. A., Aleksandrova, G. P., Feoktistova, L. P., Sapozhnikov, A. N., Sukhov, B. G., et al. (2006). Redox reactions of arabinogalactan with silver ions and formation of nanocomposites. *Russian Journal of General Chemistry (English Translation)*, *76*, 1111–1116.

Grischenko, L. A., Parshina, L. N., Kanitskaya, L. V., Larina, L. I., Novikova, L. N., & Trofimov, B. A. (2013). Propargylation of arabinogalactan with propargyl halides – A facile route to new functionalized biopolymers. *Carbohydrate Research*, *376*, 7–14.

Hong, V., Presolski, S. I., Ma, C., & Finn, M. G. (2009). Analysis and optimization of copper-catalyzed azide–alkyne cycloaddition for bioconjugation. *Angewandte Chemie International Edition*, *48*, 9879–9883.

Jones, R. (1949). Studies on imidazole compounds. A synthesis of imidazoles with functional groups in the 2-position. *Journal of the American Chemical Society*, *71*, 383–386.

Kagan, S., Ickowicz, D., Shmuel, M., Altschuler, Y., Sionov, E., Pitusi, M., et al. (2012). Toxicity mechanisms of amphotericin B and its neutralization by conjugation with arabinogalactan. *Antimicrobial Agents and Chemotherapy*, *56*, 5603–5611.

Koschella, A., Richter, M., & Heinze, T. (2010). Novel cellulose based polyelectrolytes synthesized via the click reaction. *Carbohydrate Research*, *34*, 1028–1033.

Kulbokaite, R., Ciuta, G., Netopilik, M., & Makuska, R. (2009). N-PEG'ylation of chitosan via "click chemistry" reactions. *Reactive and Functional Polymers*, *69*, 771–778.

Lallana, E., Fernandez-Megia, E., & Riguera, R. (2009). Surpassing the use of copper in the click functionalization of polymeric nanostructures: A strain-promoted approach. *Journal of the American Chemical Society*, *131*, 5748–5750.

Lallana, E., Riguera, R., & Fernandez-Megia, E. (2011). Reliable and efficient procedures for the conjugation of biomolecules through Huisgen azide–alkyne cycloadditions. *Angewandte Chemie International Edition*, *50*, 8794–8804.

Lallana, E., Sousa-Herves, A., Fernandez-Trillo, F., Riguera, R., & Fernandez-Megia, E. (2012). Click chemistry for drug delivery nanosystems. *Pharmaceutical Research*, *29*, 1–34.

Laurent, S., Forge, D., Port, M., Roch, A., Robic, C., Elst, L. V., et al. (2008). Magnetic iron oxide nanoparticles: Synthesis, stabilization, vectorization, physicochemical characterizations, and biological applications. *Chemical Reviews*, *108*, 2064–2110.

Liang, L., & Astruc, D. (2011). The copper(I)-catalyzed alkyne-azide cycloaddition (CuAAC) "click" reaction and its applications. An overview. *Coordination Chemistry Reviews*, *255*, 2933–2945.

Liebert, T., Hänsch, C., & Heinze, T. (2006). Click chemistry with polysaccharides. *Macromolecular Rapid Communications*, *27*, 208–213.

López-Franco, Y., Higuera-Ciapara, I., Goycoolea, F. M., & Wang, W. (2009). Other exudates: Tragancanth, karaya, mesquite gum and larchwood arabinogalactans. In G. O. Phililips, & P. A. Williams (Eds.), *Handbook of hydrocolloids* (pp. 495–534). Cambridge: Woodhead Publishing Ltd.

Mahdavi, M., Ahmad, M. B., Haron, M. J., Namvar, F., Nadi, B., Ab Rahman, M. Z., et al. (2013). Synthesis, surface modification and characterisation of biocompatible magnetic iron oxide nanoparticles for biomedical applications. *Molecules*, *18*, 7533–7548.

Mamidyala, S. K., & Finn, M. G. (2010). *In situ* click chemistry: Probing the binding landscapes of biological molecules. *Chemical Society Reviews*, *39*, 1252–1261.

Meldal, M. (2008). Polymer "clicking" by CuAAC reactions. *Macromolecular Rapid Communications*, *29*, 1016–1051.

Meldal, M., & Tornøe, C. W. (2008). Cu-catalyzed azide–alkyne cycloadditions. *Chemical Reviews*, *108*, 2952–3015.

Miller, A. R. (1986). Oxidation cell wall polysaccharides by hydrogen peroxides: A potential mechanism for cell wallbreakdown in plants. *Biochemical and Biophysical Research Communications*, *141*, 238–244.

Mjos, K. D., & Orvig, C. (2014). Metallodrugs in medicinal inorganic chemistry. *Chemical Reviews*, *114*, 4540–4563.

Nakagawa, A., Kamitakahara, H., & Takano, T. (2012). Synthesis and thermoreversible gelation of diblock methylcellulose analogues via Huisgen 1,3-dipolar cycloaddition. *Cellulose*, *19*, 1315–1326.

Oliveira, J. R., Martins, M. C., Mafra, L., & Gomes, P. (2012). Synthesis of O-alkynyl-chitosan and its chemoselective conjugation with a PEG-like amino-azide through click chemistry. *Carbohydrate Polymers*, *87*, 240–249.

Parshina, L. N., Tantsyrev, A. P., Grishchenko, L. A., & Trofimov, B. A. (2013). Nanosized Pd(0)-arabinogalactan composites as catalysts in the Sonogashira reaction. *Russian Journal of Organic Chemistry (English Translation)*, *49*, 412–416.

Pawar, R. P., Kushekar, B. A., Jadhav, B. S., Kharat, K. R., Borade, R. M., & Domb, A. J. (2011). Arabinogalactan in clinical use. In A. J. Domb, N. Kumar, & A. Ezra (Eds.), *Biodegradable polymers in clinical use and clinical development* (pp. 217–245). Hoboken, NJ: John Wiley & Sons.

Peng, P., Cao, X., Peng, F., Bian, J., Xu, F., & Sun, R. (2012). Binding cellulose and chitosan via click chemistry: Synthesis, characterization, and formation of some hollow tubes. *Journal of Polymer Science, Part A: Polymer Chemistry*, *50*, 5201–5210.

Pinhassi, R. I., Assaraf, Y. G., Farber, S., Stark, M., Ickowicz, D., Drori, S., et al. (2010). Arabinogalactan–folic acid–drug conjugate for targeted delivery and target-activated release of anticancer drugs to folate receptor-overexpressing cells. *Biomacromolecules*, *11*, 294–303.

Pohl, M., Michaelis, N., Meister, F., & Heinze, T. (2009). Biofunctional surfaces based on dendronized cellulose. *Biomacromolecules*, *10*, 382–389.

Polyakov, N. E., Magyar, A., & Kispert, L. D. (2013). Photochemical and optical properties of water-soluble antioxidants: Aggregation vs complexation. *Journal of Physical Chemistry B*, *117*, 10173–10182.

Raso, G. M., Simeoli, R., Iacono, A., Santoro, A., Amero, P., Paciello, O., et al. (2014). Effects of a *Lactobacillus paracasei* B21060 based synbiotic on steatosis, insulin signaling and toll-like receptor expression in rats fed a high-fat diet. *Journal of Nutritional Biochemistry*, *25*, 81–90.

Riede, L., Grube, B., & Gruenwald, J. (2013). Larch arabinogalactan effects on reducing incidence of upper respiratory infections. *Current Medical Research and Opinion*, *29*, 251–258.

Robinson, R. R., Feirtag, J., & Slavin, J. L. (2001). Effect of dietary arabinogalactan on gastrointestinal and blood parameters in healthy human subjects. *Journal of the American College of Nutrition*, *20*, 279–285.

Rostovtsev, V. V., Green, L. G., Fokin, V. V., & Sharpless, K. B. (2002). A stepwise Huisgen cycloaddition process: Copper(1)-catalyzed regioselective "Ligation" of azides and terminal alkynes. *Angewandte Chemie International Edition*, *41*, 2596–2599.

Shostakovsky, M. F., Skvortsova, G. G., Glazkova, N. P., & Domnina, E. S. (1969). *Khimiya Geterotsiklicheskikh Soedinenii*, 1070–1072, *Chemical Abstracts, 72*, 132612.

Shurygina, I. A., Sukhov, B. G., Fadeeva, T. V., Umanets, V. A., Shurygin, M. G., Ganenko, T. V., et al. (2011). Bactericidal action of Ag(0)-antithrombotic sulfated arabinogalactan nanocomposite: Coevolution of initial nanocomposite and living microbial cell to a novel non-living nanocomposite. *Nanomedicine: NBM*, *7*, 827–833.

Such, G. K., Johnston, A. P. R., Liang, K., & Caruso, F. (2012). Synthesis and functionalization of nanoengineered materials using click chemistry. *Progress in Polymer Science*, *37*, 985–1003.

Sukhov, B. G., Aleksandrova, G. P., Grishchenko, L. A., Feoktistova, L. P., Sapozhnikov, A. N., Proidakova, et al. (2007). Nanobiocomposites of noble metals on arabinogalactan basis: Synthesis and structure. *Journal of Structural Chemistry (English Translation)*, *48*, 922–927.

Tahir, M. N., Lämmerhardt, N., & Mischnick, P. (2012). Introduction of various functionalities into polysaccharides using alkynyl ethers as precursors: Pentynyl dextrans. *Carbohydrate Polymers*, *88*, 154–164.

Thirumurugan, P., Matosiuk, D., & Jozwiak, K. (2013). Click chemistry for drug development and diverse chemical–biological applications. *Chemical Reviews*, *113*, 4905–4979.

Tornøe, C. W., Christensen, C., & Meldal, M. (2002). Peptidotriazoles on solid phase: [1,2,3]-Triazoles by regiospecific copper(I)-catalyzed 1,3-dipolar cycloadditions of terminal alkynes to azides. *Journal of Organic Chemistry*, *67*, 3057–3064.

Trofimov, B. A., Parshina, L. N., & Grishchenko, L. A. (2011). *Method for production of arabinogalactan propargyl ether*. R.F. Patent 2 425 843; *Chemical Abstracts, 155*, 274091.

Trofimov, B. A., Sukhov, B. G., Aleksandrova, G. P., Medvedeva, S. A., Grishchenko, L. A., Mal'kina, A. G., et al. (2003). Nanocomposites with magnetic, optical, catalytic and biologically active properties based on arabinogalactan. *Doklady Chemistry (English Translation)*, *393*, 287–288.

Trofimov, B. A., Sukhov, B. G., Nosyreva, V. V., Mal'kina, A. G., Aleksandrova, G. P., & Grishchenko, L. A. (2007). Pd(0)-arabinogalactan nanocomposites as catalysts for dimerization of acetylenic. *Doklady Chemistry (English Translation)*, *417*, 261–263.

Udani, J. K. (2013). Immunomodulatory effects of ResistAid^{TM}: A randomized, double-blind, placebo-controlled, multidose study. *Journal of the American College of Nutrition*, *32*, 331–338.